Spin canting and hyperfine interactions in the reentrant Ising spin glass $Fe_{0.62}Mn_{0.38}TiO_3$

1993 J. Phys.: Condens. Matter 5 615

(http://iopscience.iop.org/0953-8984/5/5/012)

J. Phys.: Condens. Matter 5 (1993) 615–622. Printed in the UK

Spin canting and hyperfine interactions in the re-entrant Ising spin glass $Fe_{0.62}Mn_{0.38}TiO_3$

A Seidel†, K Gunnarsson‡, L Häggström†, P Svedlindh‡, H Aruga Katori§ and A Ito||

† Department of Physics, Uppsala University, Box 530, S-751 21 Uppsala, Sweden
‡ Department of Technology, Uppsala University, Box 534, S-751 21 Uppsala, Sweden
§ Institute for Solid State Physics, University of Tokyo, Roppongi, Minato-ku, Tokyo 106, Japan
|| Ochanomizu University, Department of Physics, Bunkyo-ku, Tokyo 112, Japan

Received 14 September 1992, in final form 9 November 1992

Abstract. The re-entrant Ising spin glass $Fe_{0.62}Mn_{0.38}TiO_3$ has been studied with Mössbauer spectroscopy as well as with field-cooled and zero-field-cooled magnetization measurements. The Néel and spin glass temperatures obtained are $T_N = 32.8$ K and $T_g = 25.8$ K, respectively. The ^{57}Fe Mössbauer spectra recorded below 32 K are described in terms of two subspectra emanating from paramagnetic iron atoms and from iron atoms with canted magnetic moments. The canting angle was determined to be $\theta \simeq 45°$ for all temperatures below T_N. The intensity of the paramagnetic subspectrum decreases with decreasing temperature and is typically about 25% at T_g. Longitudinal as well as transverse re-entrant spin glass behaviour is observed in magnetization measurements.

1. Introduction

The ilmenites $FeTiO_3$ and $MnTiO_3$ have corundum type crystal structures with Fe^{2+}/Mn^{2+} and Ti^{4+} in equivalent octahedral sites of the HCP oxygen lattice. The structure is shown in figure 1. The cations form honeycomb patterns in alternate layers in the hexagonal c plane. Every third octahedral site along c is vacant. The cations sites have a trigonal symmetry axis along c. The crystalline field and spin–orbit coupling cause a strong magnetic anisotropy of the Fe^{2+} ions with c as the spin easy axis. Actually, a small canting angle of $1.60 \pm 0.1°$ of the magnetic moments to the c axis has been found in $FeTiO_3$ [1]. Dipole–dipole interaction causes c to be the easy axis in $MnTiO_3$ also [2]. The interplane coupling is antiferromagnetic in both compounds while the intralayer order is ferromagnetic in $FeTiO_3$ and antiferromagnetic in $MnTiO_3$. The magnetic coupling between adjacent c planes is small but not negligible. The exchange constant between nearest Fe neighbours of different planes in $FeTiO_3$ has been reported to be -55% of the value for neighbours in the same plane [3].

In a mixed compound $Fe_xMn_{1-x}TiO_3$, the Fe and Mn ions are randomly distributed on the Fe/Mn cationic sites, and their spins experience exchange frustrations leading to spin glass (SG) behaviour in the samples with $0.39 < x < 0.57$ [4, 5]. In the single crystal $Fe_{0.62}Mn_{0.38}TiO_3$ which was studied here, the SG

0953-8984/93/050615+08$07.50

ordering coexists with non-perfect antiferromagnetic (AF) order below the spin glass temperature T_g [6]. The system is a so-called re-entrant SG (RSG), meaning $T_N > T_g$.

The aim of this study was to compare changes in the hyperfine interactions at T_g with results from magnetization measurements. We expected an abrupt decrease of the spin alignment on entering the SG state. Such a drop in the spin alignment at T_g, due to the freezing of the transverse spin component, has been found in the metallic spin glass $Au_{0.832}Fe_{0.168}$ by Lange *et al* [7] and in PdFeMn by Takeda *et al* [8], and non-collinear spin arrangement has been suggested to appear below T_g in short-range insulating spin glasses from simulations on re-entrant planar ferromagnets by Saslow and Parker [9].

2. Experimental details

The magnetization measurements were made in a superconducting quantum interference device (SQUID) magnetometer. The zero-field-cooled (ZFC) magnetization was obtained by cooling the sample in zero field from $T = 60$ K to 5 K. A static field in the range 0.05 kG $< H <$ 12 kG was then applied parallel/perpendicular to the c axis and the temperature was increased stepwise; at each temperature the longitudinal/transverse ZFC magnetization M_{ZFC} was recorded. After reaching $T = 60$ K, the temperature was decreased stepwise and the field-cooled magnetization M_{FC} measured. A low cooling rate was used, in order for $\chi_{FC} = M_{FC}/H$ to be approximately equal to the static susceptibility.

Mössbauer measurements were made with a ^{57}CoRh source at room temperature. A 0.10 ± 0.02 mm thick $Fe_{0.62}Mn_{0.38}TiO_3$ single crystal was used as absorber in conventional transmission geometry, with the γ radiation in the crystallographic c direction. This absorber has an effective Mössbauer thickness $D \simeq 4$, calculated as $D = fNd\sigma$, where N is the number of ^{57}Fe atoms cm^{-3} in the absorber, d is the thickness in cm, σ is the resonance cross section and the absorber factor f has been estimated to 0.6. Simultaneous α-Fe calibration spectra were taken in the opposite direction. A liquid He flow cryostat was used to obtain sample temperatures from 10 K to 37 K. The temperature was kept constant within ± 1 K. All spectra were analysed using a Mössbauer analysis program with a complete transmission integral calculation [10] to correct for the finite absorber thickness. A complete combined interaction Hamiltonian was used in the program for electric quadrupole and magnetic interactions of comparable strengths.

3. Results and interpretation

3.1. Magnetization

Figure 2 shows χ_{ZFC} and χ_{FC} versus temperature, measured with the field applied parallel and perpendicular to the c axis. The cusp in χ indicates the phase transition between the paramagnetic (PM) and the AF states. The temperatures at which χ_{ZFC} differs from χ_{FC} form the temperature range where a fraction of the frustrated magnetic moments are frozen. Irreversibility in χ appears in the transverse as well as in the longitudinal direction, but the transverse component is about 20% of the magnitude of the longitudinal. The anisotropy of the magnetization, being very large already in the PM phase, shows that the magnetocrystalline anisotropy energy is larger

than the exchange energies. The Néel temperature is $T_N = 32.8 \pm 0.2$ K. The spin glass temperature determined by AC susceptibility measurements is $T_g = 25.8 \pm 0.4$ K [11].

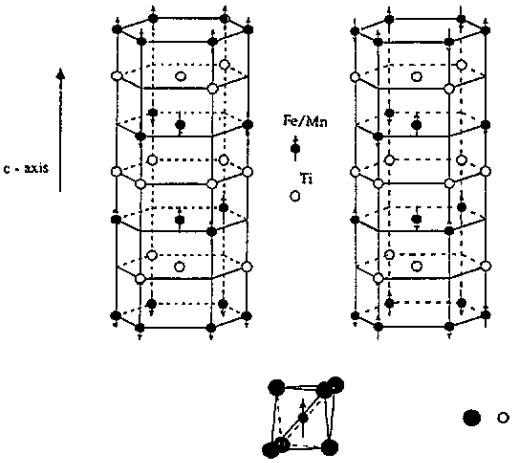

Figure 1. Hexagonal structure of the ilmenites $FeTiO_3$ and $MnTiO_3$: above, the cation sublattice only; below, the oxygen nearest neighbour arrangement.

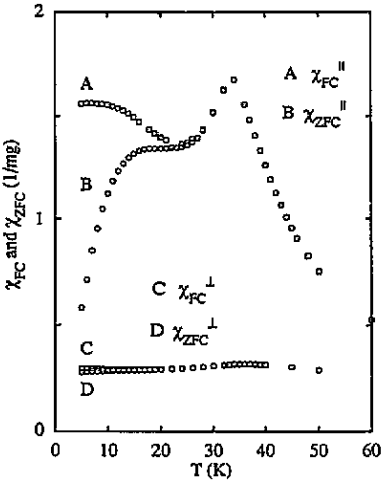

Figure 2. Longitudinal and transverse field-cooled (FC) and zero-field-cooled (ZFC) magnetic susceptibilities of $Fe_{0.62}Mn_{0.38}TiO_3$.

In the anisotropic spin glass Fe_2TiO_5, Yeshurun and Sompolinsky [12] have stated that χ along the crystallographic a/b axes shows some anomaly associated with a spin glass transition. The transverse irreversibility was found to be an order of magnitude weaker than the longitudinal one. In $Fe_{0.62}Mn_{0.38}TiO_3$, we find a re-entrant spin glass behaviour in the transverse as well as in the longitudinal direction, although a factor of $\frac{1}{5}$ lower in susceptibility.

The possibility of a misalignment of the sample during the measurement has been considered. For this reason a series of experiments was made where the angles between the sample, pick-up coils and applied fields were carefully checked. However, in analysing these results, it was found that the misalignment angle would be as large as 10° or more in order to account for the magnitude of the irreversibility in the transverse component.

3.2. Mössbauer spectroscopy

In figure 3 the ^{57}Fe Mössbauer spectra of the $Fe_{0.62}Mn_{0.38}TiO_3$ single crystal are shown. The hyperfine parameters obtained at 10 K and 295 K are listed in table 1.

For $T > T_N$ the spectra are quadrupole split doublets with rather narrow lines at room temperature ($\Gamma_{obs} = 0.31$ mm s^{-1}) and slightly broadened at 37 K ($\Gamma_{obs} = 0.37$ mm s^{-1}). For pure $FeTiO_3$ and $MnTiO_3$ the point group symmetry of the Fe (Mn) site requires the nuclear electric field gradient to be axially symmetric with the principal axis z parallel to c. The area ratio of the two lines in Fe-ilmenite should then be 1:3 with the principal component of the electric field gradient (EFG) tensor V_{zz} positive and parallel with the γ direction [15], i.e. parallel to c [16]. In this way we would expect the polar angle θ between the z axis of the EFG and B_{hf} to

Table 1. Values of the hyperfine parameters at 10 K and at 295 K obtained in this study together with values from polycrystalline material reported by Syono *et al* [13] and Grant *et al* [14]. The CS is given relative to natural iron at room temperature. The quadrupole splitting is defined as $dQ = eQV_{zz}/2$ and B_{hf} is the magnetic hyperfine field.

Compound	T (K)	CS (mm s^{-1})	dQ (mm s^{-1})	B_{hf} (T)	
$Fe_{0.62}Mn_{0.38}TiO_3$	295	1.09 ± 0.01	0.76 ± 0.01	0.0	
	10	1.22 ± 0.02	1.55 ± 0.03	6.3 ± 0.1	CM
		1.23 ± 0.02	1.58 ± 0.06	0.0	PM
$FeTiO_3$ [13]	300	1.08	0.7		
	4.2		1.44	5.6	
$MnTiO_3(^{57}Fe)$ [13]	300	1.11	0.8		
	4.2		1.62	3.3	
$FeTiO_3$ [14]	5	1.22 ± 0.01	1.44 ± 0.01	4.3 ± 0.3	

be identical to the angle between c and B_{hf}. For our mixed sample the point group symmetry of the Fe site is disturbed due to the substitution of Mn for Fe. In any case, taking only the nearest O atom into account, the EFG tensor for the lattice would still be axially symmetric with the c and z axes parallel. In the analysis below we have assumed this to be the case for the full EFG tensor although a slight deviation of the parallelism and axial symmetry cannot be excluded.

The spectra for $T < T_N$ are broad unresolved patterns typical for a disordered material. Broadening of this kind can be a consequence of distributions in the values of the hyperfine parameters (the magnetic hyperfine field B_{hf}, the central shift CS and the quadrupole splitting $dQ = eQV_{zz}/2$ with Q denoting the nuclear quadrupole moment) or by a distribution in the polar angle θ between the principal axes of the EFG and B_{hf}. Another explanation of broadening can be the existence of magnetic relaxation times, τ, of the same order of magnitude as the Larmor precession time of the Mössbauer nuclear level: $\sim 10^{-7}$ s in $Fe_{0.62}Mn_{0.38}TiO_3$.

The SG is characterized by a spectrum of relaxation times ranging from microscopic times to a maximum value, τ_{max}, which diverges on approaching T_g from above. Microscopically, the SG can be pictured as a collection of atomic magnetic moments, each having a certain arrangement of neighbours and a certain probability per unit time of flipping. Taking not only nearest neighbours into consideration, there will be a large number of possible configurations.

Using this picture, the spectra can be treated as superpositions of subspectra with different hyperfine parameters. It is possible that a PM subspectrum coexists with the magnetically split absorption patterns, at least at temperatures close to T_N. In this model, a PM subspectrum is created by magnetic moments with relaxation times smaller than the Larmor precession time of the Mössbauer level. Judging from the narrow lines of the high-temperature doublet we can assume that the CS is almost the same for all subspectra at low temperatures also.

In analysing this type of Mössbauer spectrum one is obliged to restrict the number of variables and to use simplified models in the fitting. It turned out to be possible to obtain reasonably good fits to the low-temperature spectra when subspectra arising from canted (CM) and PM moments were used in the least squares fit. Introducing also a subspectrum arising from non-canted or longitudinal moments (LM) gave only minor improvements to the fits. Furthermore the intensity of this LM subspectrum turned out to be rather low and therefore not so critical in the interpretation of the data. The following model was used. Basically, the spin system has an $FeTiO_3$ type AF

order. A fraction of the atomic magnetic moments is frustrated and will minimize the total energy by changing its orientation away from c, decreasing the alignment also among the neighbouring spins. Effects of relaxation and variations in the hyperfine parameters due to a variation in magnetic neighbour arrangement are to some extent covered by broadening of the individual lines in the analysis.

Finally, the fitting procedure used the following assumptions. Each spectrum was described with one electric quadrupole split doublet (the PM subspectrum) and one magnetically and electrically split subspectrum emanating from canted moments (the CM subspectrum). Their relative intensities, the Lorentzian line widths and the quadrupole coupling constants for the subspectra were allowed to vary freely, as well as the magnetic hyperfine fields and the canting angle for the canted subspectra. One restriction was that all subspectra must have identical values of CS and that the asymmetry found in the doublet at 37 K should be roughly preserved for the PM subspectrum below 37 K. A small misalignment of the c axis of the single crystal and/or a small misalignment of the z axis of the EFG tensor with respect to the incoming γ rays were also allowed in the fitting.

The relative intensities versus temperature of the CM and PM subspectra which give the best least squares fits are plotted in figure 4. The angle θ of the CM subspectrum varies between 43° and 47° with an average around 45°. At $T = 30$ K the intensity of the CM subspectrum is already dominant with roughly $\frac{2}{3}$ of the total intensity.

The temperature dependence of the intensities follows the expected behaviour. The PM intensity grows from a value of 5% at 10 K at the expense of the CM intensity. The frustrated spins, having the smallest total exchange fields, are easily thermally excited. With decreasing temperature the frustrated spins freeze at some large angle to c and will have an increasing influence on the spin system thereby causing a misalignment of the neighbouring magnetic moments. Our interpretation is that for temperatures $T < T_N$ the PM subspectrum will arise mainly from frustrated spins, 'leaving' the canted state when the temperature increases.

The angle θ of the hyperfine fields with respect to the c axis is roughly 45°, a large value considering the anisotropy in χ and the strong crystal field anisotropy of Fe^{2+} in $FeTiO_3$. A mean canting angle of $\langle\theta\rangle \simeq 60°$ has been observed in the non-re-entrant $Fe_{0.5}Mn_{0.5}TiO_3$ [17–19].

In figure 5 the hyperfine field B_{hf} is plotted versus temperature. The low values of B_{hf} at low T show that the iron orbital angular momentum is unquenched as expected for Fe^{2+} in a uniaxial crystal field making an orbital doublet lower. However, compared to B_{hf} in the ordered Fe and Mn ilmenites (see table 1), at 10 K our canted values of −6.3 T (assumed to be negative) are larger in magnitude. Calculated values for the contributions to B_{hf} for Fe-ilmenite as reported by Grant *et al* [14] are $B_{orbital} = +42.0$ T, $B_{dipolar} = +5.9$ T and $B_{Fermi} = -52.2$ T giving $B_{hf} = -4.3$ T. Possible explanations for our larger value are that the orbital and the dipolar contributions to B_{hf} are dependent on the canting angle of the magnetic moment.

The orbital level scheme and the electronic wave functions of Fe^{2+} in a crystalline field of trigonal symmetry has been discussed by Okiji and Kanamori [20]. The lowest level turned out to be a doublet. An almost linear relation between $B_{3d} = B_{dipolar} + B_{orbital}$ and $dQ_{valence}$ was found for these types of compounds. Assuming the lattice contribution to the EFG to be small, this shows that the value of B_{3d} is less positive for the Fe in $FeTiO_3$ than for Fe in the CM subspectrum of our sample. Hence, we should expect a more negative value for the total magnetic

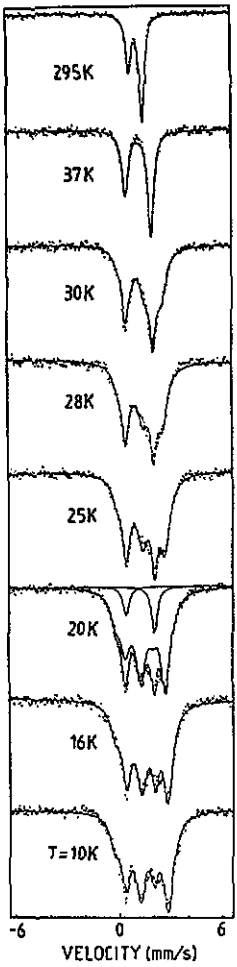

Figure 3. Mössbauer spectra of $Fe_{0.62}Mn_{0.38}TiO_3$ at various temperatures. The solid lines are the best fits to the model described in the text. The PM and CM subspectra are displayed in the spectra recorded at 20 K.

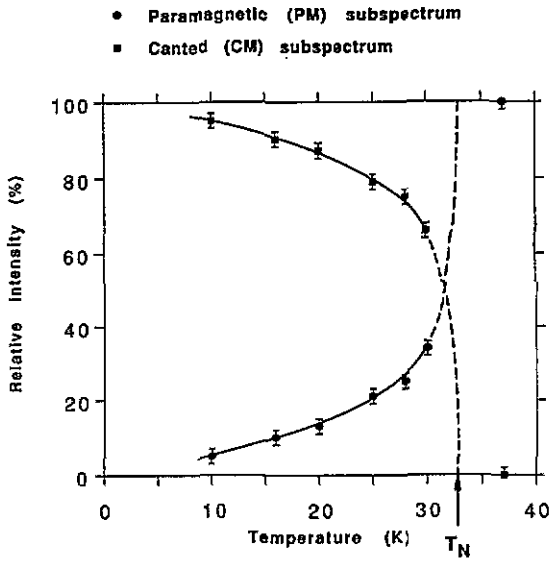

Figure 4. Relative intensities of the Mössbauer subspectra attributed to frozen iron magnetic moments canted relative to the crystallographic c axis, and paramagnetic iron moments.

hyperfine field in $FeTiO_3$ than for the CM subspectrum which is contradictory to our observations. It is therefore tempting to also assume changes in the term B_{Fermi} for Fe in $FeTiO_3$ relative to $Fe_{0.62}Ti_{0.38}O_3$ as a result of the canting angles of Fe^{2+} spins.

The EFG is large with a dominating orbital contribution due to the strong anisotropy. This gives a large splitting. As we can see in figure 6, dQ decreases with temperature, which can be attributed to the increase of populations on the higher electronic states with small dQ and negative dQ [21]. There is also an effect of the change in the mean square displacements of atoms in the crystal lattice [22]. Below T_N the fittings gave two values for dQ, from the PM and CM subspectra respectively for each spectrum. The difference is typically ~ 0.03 mm s^{-1} or within limits of error the values are the same. In figure 6 the average values are plotted. The type of spin angular dependence on dQ reported by Fujita *et al* [23] could not be observed

below T_N in our case. The values of dQ for the PM subspectrum obtained in this investigation fall very nicely in between the values reported for $FeTiO_3$ and $MnTiO_3$ (see table 1).

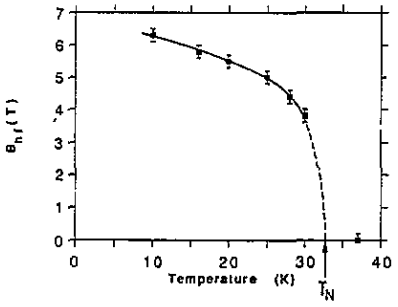

Figure 5. Hyperfine fields for the canted subspectrum versus T for $Fe_{0.62}Mn_{0.38}TiO_3$.

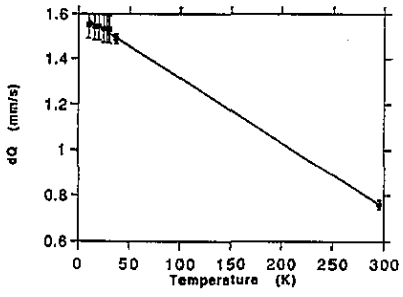

Figure 6. Quadrupole splitting versus temperature for $Fe_{0.62}Mn_{0.38}TiO_3$.

The room temperature value of the CS is close to what has been found for $FeTiO_3$ (see table 1) and is typical for high-spin Fe^{2+} with a low degree of covalency [24].

4. Discussion and conclusions

It can be argued that a rough analysis of this kind of Mössbauer spectra from a magnetically disordered material might yield spurious results. The model with two subspectra described above was therefore checked using a more detailed analysis allowing for a distribution in canting angles and in magnetic hyperfine fields. It turns out that the results of the simplified model (in terms of hyperfine parameters and relative intensities) agree with the more detailed model. Our argument for presenting the simpler model is that the number of parameters ought to be kept to a minimum in analysing poorly resolved spectra.

The freezing temperature, T_f, below which dynamic effects are observed, is dependent on the timescale of observation. At a certain temperature the SG system is characterized by a range of relaxation times from zero to a temperature dependent maximum relaxation time, τ_{max}, which diverges on approaching T_g from above. At T_f the observation time of the experimental probe is $t = \tau_{max}$. Dynamic scaling analysis, using AC susceptibility data [25], yields $T_f \simeq 33$ K for $t = 10^{-7}$ s, which is the observation time of the Mössbauer measurement. Thus, the freezing temperature in the Mössbauer measurement is approximately the same as T_N.

The Mössbauer and the magnetization results can be explained consistently by the fact that the strong uniaxial anisotropy of the Ising system is overcome locally by the competing exchange fields, but the resulting canting of the spins has projections on the c plane distributed in all directions. The net response to transverse magnetic fields, the transverse susceptibility, remains small in spite of the large canting angles.

It has been confirmed in this study that there is a large average canting angle of the magnetic moments in the re-entrant Ising spin glass $Fe_{0.62}Mn_{0.38}TiO_3$. Furthermore no obvious effects of the re-entrant transition could be seen in the results of the data analysis. However, Mössbauer measurements on RSGs having a larger difference between T_N and T_f may show more obvious effects of re-entrance.

The advantages with the Mössbauer method in studies of dynamic systems is the short observation time (of the order of 10^{-7} s in ^{57}Fe) and the possibility of obtaining angular information about the atomic magnetic moments from the spectra without the application of an external magnetic field. However, it is necessary to have a plausible microscopical model for the spin system to be able to restrict the number of free parameters in the analysis. Only then it will be possible to obtain unambiguous information from the unresolved spectra.

Acknowledgments

KG and PS acknowledge funding from the Swedish Natural Science Research Council (NFR).

References

[1] Yamaguchi Y, Kato H, Takei H, Goldman A I and Shirane G 1986 *Solid State Commun.* **59** 865–8
Kato H, Yamaguchi Y, Ohashi M, Yamada M, Takei H and Funahashi S 1983 *Solid State Commun.* **45** 669–72
[2] Goodenough J B and Stickler J J 1967 *Phys. Rev.* **164** 768–78
[3] Kato H, Funahashi S, Yamaguchi Y, Yamada M and Takei H 1983 *J. Magn. Magn. Mater.* **31–4** 617–18
[4] Ito A, Aruga H, Torikai E, Kikuchi M, Syono Y and Takei H 1986 *Phys. Rev. Lett.* **57** 483
[5] Ito A, Aruga H, Kikuchi M, Syono Y and Takei H 1988 *Solid State Commun.* **66** 475
[6] Yoshizawa H, Mitsuda S, Aruga H and Ito A 1989 *J. Phys. Soc. Japan* **58** 1416–26
[7] Lange S, Abd-Elmeguid M M and Micklitz H 1990 *Phys. Rev.* B **41** 6907–12
[8] Takeda Y, Morimoto S, Ito A, Sato T and Miyako Y 1985 *J. Phys. Soc. Japan* **54** 2000
[9] Saslow W M and Parker G 1986 *Phys. Rev. Lett.* **56** 1074–7
[10] Jernberg P and Sundqvist T 1983 *University of Uppsala Internal Report UUIP-1090*
[11] Gunnarsson K, Andersson J-O, Svedlindh P, Nordblad P, Lundgren L, Aruga H and Ito A 1991 *Proc. Int. Conf. on Magnetism, Edinburgh* (Amsterdam: North-Holland)
[12] Yeshurun Y and Sompolinsky H 1985 *Phys. Rev.* B **31** 3191
[13] Syono Y, Ito A and Morimoto S 1981 *J. Phys. Chem. Solids* **42** 483–6
[14] Grant R W, Housley R M and Geller S 1972 *Phys. Rev.* B **5** 1700–3
[15] Zory P 1965 *Phys. Rev.* **140** A1401
[16] Garg V K and Puri S P 1971 *Phys. Status Solidi* b **44** K45–7
[17] Ito A, Aruga H, Morimoto S and Yoshizawa H 1988 *J. Physique* C8 1129–30
[18] Ito A, Morimoto S and Aruga H 1990 *Hyperfine Interact.* **54** 567
[19] Ito A, Torikai E, Morimoto S, Aruga H, Kikuchi M, Syono Y and Takei H 1990 *J. Phys. Soc. Japan* **59** 829–32
[20] Okiji A and Kanamori J 1964 *J. Phys. Soc. Japan* **19** 908–15
[21] Ingalls R 1964 *Phys. Rev.* **133** A787
[22] Nishiyama K and Riegel D 1978 *Hyperfine Interact.* **4** 490
[23] Fujita T, Ito A and Ono K 1969 *J. Phys. Soc. Japan* **27** 1143
[24] Ingalls R, van der Woude F and Sawatzky G A 1978 *Mössbauer Isomer Shifts* ed G K Shenoy and F E Wagner (Amsterdam: North Holland) ch 7, p 364
[25] Gunnarsson K, Svedlindh P, Nordblad P, Lundgren L, Aruga H and Ito A 1988 *Phys. Rev. Lett.* **61** 754